P10.3 MOBILE, DUAL-DOPPLER ANALYSIS OF TORNADOGENESIS: THE 15 MAY 2003 SUPERCELL IN SHAMROCK, TEXAS

Michael M. French*
Howard B. Bluestein
School of Meteorology, University of Oklahoma, Norman, Oklahoma

David C. Dowell
Cooperative Institute for Mesoscale Meteorological Studies, Norman, Oklahoma

Louis J. Wicker
National Severe Storms Laboratory, Norman, Oklahoma

Matthew R. Kramar
NOAA/NWS, Amarillo, Texas

Andrew L. Pazmany
Prosensing, Amherst, Massachusetts

1. INTRODUCTION

Gaining a detailed understanding of tornadogenesis in supercell thunderstorms is severely limited by the inability to observe the process consistently at a close distance. However, the capacity to collect observational data of tornadogenesis has increased greatly in the past ten years due to the advancement of mobile Doppler radar systems. More specifically, the use of dual-Doppler analysis techniques can provide fine-scale observations of wind fields in supercell thunderstorms. These studies use several methods to obtain dual-Doppler data of supercells.

Early attempts at collecting dual-Doppler datasets required a supercell to pass through an area where two non-mobile, Doppler research radars were located (e.g. Brandes 1978; Dowell and Bluestein 1997). Later attempts, during projects such as VORTEX, fitted airplanes with Doppler radars to obtain pseudo-dual-Doppler data as the planes flew in the vicinity of supercells (e.g. Wakimoto and Atkins 1996; Wakimoto et al. 1998; Wakimoto and Liu 1998; Ziegler et al. 2001; Dowell and Bluestein 2002; Wakimoto et al. 2003). Unfortunately, supercell passes through a non-mobile network of radars are rare and require a great deal of good luck. Furthermore, the non-mobile radars were widely spaced, thereby limiting the spatial resolution of the data. On the other hand, airborne radars experience significant ground clutter contamination near the surface, and traverses near the storm are separated by as much as five to ten minutes. This time separation makes a detailed study of a rapidly evolving tornado very difficult (Bluestein et al. 2003).

Perhaps the most successful and promising of these methods for obtaining tornadogenesis data are mobile, Doppler radars mounted on ground-based vehicles. As it became apparent by the mid-1990s that such radars were a viable way to obtain Doppler radar data in supercells, it was suggested first that one radar could be used to obtain pseudo-dual-Doppler data by moving the radar parallel to the motion of the tornado (Bluestein et al. 1994). Then, the idea of using multiple mobile, ground-based, Doppler radars to obtain a dual-Doppler wind field was suggested (Bluestein et al. 1995; Wurman et al. 1997). Since then, these radars have been used to assess the wind field near the ground in tornadoes and low-level mesocyclones at a much finer resolution than by previous methods (e.g., Bluestein and Pazmany 2000; Wurman and Gill 2000; Burgess et al. 2002; Wurman 2002; Bluestein et al. 2003). Ideally, multiple (two or more) mobile, Doppler radars would obtain data of the same tornadic supercell.

In such a case, a dual-Doppler analysis could present a comprehensive look at the low-level mesocyclone and perhaps even the tornado itself with finer spatial and temporal resolution than is possible with non-mobile Doppler radars and airborne Doppler radars. Furthermore, a dual-Doppler analysis of tornadogenesis could provide a particularly useful map of the wind field before, during, and after the formation of a tornado near

* *Corresponding author address:* Michael M. French; Univ. of Oklahoma, School of Meteorology; 100 E. Boyd, Rm. 1310; Norman, OK 73019; e-mail: mfrench@ou.edu .

the ground. As a result, this analysis could lead to a better understanding not only of the structure of a tornado but also of the environments that are conducive for tornado formation and those that are not, in effect, figuring out why tornadoes form (Bluestein 1999).

As mobile, ground-based, Doppler radars increase in number and improve in quality, the possibilities for dual-Doppler data acquisition of tornadogenesis increase. One such example was the case on 15 May 2003 near Shamrock, Texas. This study is a dual-Doppler analysis of a tornadic supercell from 15 May 2003 that qualitatively assesses how the analysis relates to the current understanding of tornado formation, development, and dissipation.

2. DATA COLLECTION

During the spring season of 2003, a mobile, dual-polarization, 3-cm wavelength Doppler radar (XPOL) was used to collect data near supercell thunderstorms (Pazmany et al. 2003). In addition, a mobile, Doppler, 5-cm radar (Shared Mobile Atmospheric Research and Teaching or SMART radar) was used at various times during the same time frame to collect data in convective storms (Biggerstaff and Guynes 2000). On the evening of 15 May 2003, both of these mobile radars were located south of Shamrock, Texas and scanned, in a coordinated manner, a supercell thunderstorm moving through Wheeler County, Texas.

The XPOL radar was located just outside the southern border of Shamrock and collected reflectivity, velocity, and rare dual-polarization data of the supercell thunderstorm from approximately 0240 to 0317 UTC on 16 May 2003. The SMART radar was located east of Samnorwood, Texas and collected reflectivity and velocity data of the supercell thunderstorm from 0202 to 0335 UTC on 16 May 2003. During this time period, the supercell moved through Wheeler County in the eastern Texan panhandle and later approached the Texas-Oklahoma border.

While data were being collected, a tornado formed approximately 10 km (20 km) away from the XPOL (SMART) radar. Since the sun had set by the time of apparent tornadogenesis, there could be no visual confirmation of a tornado. However, a National Weather Service (NWS) damage assessment indicates that the damage associated with the supercell was consistent with an F1 tornado. They further estimated the tornado formed at 0243 UTC in Lela, Texas (just west of Shamrock) and dissipated 29 kilometers northeast

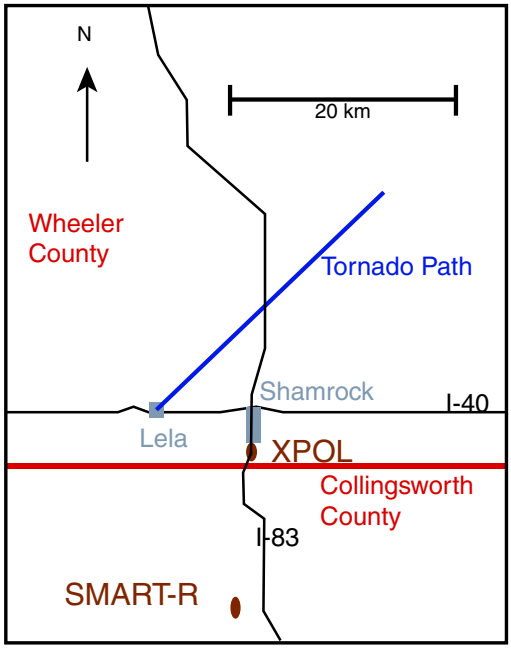

Figure 1. Diagram showing the NWS estimated tornado path and the approximate locations of the XPOL and SMART radars. The major highways and towns in the area are also depicted.

of Lela at 0320 UTC on 16 May 2003 (Fig. 1). An estimated $150,000 in damage was done in and around Lela, Texas including damaged homes, businesses, and several overturned vehicles on Interstate 40.

The Doppler velocities taken by both radars (not shown) support the formation of a tornado later than what the NWS indicated. Both radars show no discernible vortex signature until close to 0300 UTC. In any event, both radars were scanning the supercell prior to tornadogenesis. Furthermore, the NWS assessment of the location of the tornado path seems to fit qualitatively the location of the velocity couplet on both radars. Also, the indicated damage was consistent with a tornado on the ground, although the damage done to vehicles along Interstate 40 could have been caused by a rear-flank downdraft (C. Alexander, personal communication).

3. METHODOLOGY AND DATA ANALYSIS

Both sets of radar reflectivity and Doppler velocity were analyzed. The data were first edited using the SOLO software package (Nettleton et al. 1993; Oye et al. 1995). The editing consisted mainly of dealiasing radial velocities. The Nyquist

velocity for the XPOL (SMART) radar was 16.0 ms^{-1} (19.95 ms^{-1}) which led to many folds throughout both sets of data and even some double-folds in the XPOL velocities.

Additionally, it was subjectively determined that there was a fairly large area of erroneous velocity returns from the SMART radar, most likely caused by a second-trip echo. The second-trip echo probably resulted from storms to the north of the Shamrock supercell, located outside the maximum unambiguous range of the radar. Both the reflectivity and the Doppler velocities were eliminated for this area which comprised the less important northern part of the supercell and did not affect the hook echo or the corresponding vortex signature/velocity couplet.

Finally, both the reflectivity and the velocity from both radars were de-speckled and ground clutter was removed. The de-speckling removed single data points not surrounded by other data points, essentially "cleaning up" the data. The removal of ground clutter that was clearly erroneous was based upon a threshold of reflectivity in close proximity to the radar.

3.1 *Dual-Doppler Methodology*

In order to run the dual-Doppler analysis software, a number of assumptions regarding both sets of data had to be made. First, it was assumed that the XPOL radar, which does not have a leveler, was level during data collection. This was a good assumption, since any lack of level ground was compensated for by the radar operator while collecting data. Also, the exact elevation angle of the XPOL radar was not known, and for the purposes of this study, was assumed to be 0.5 degrees. It was also assumed that the SMART radar computer time was correct even though it could have been off by as much as one minute. The XPOL radar had its time calibrated when the data were initially collected. Finally, since the radars were at different ranges from the supercell and the antennas were most likely aimed at different elevation angles, the mean heights of the radar volumes were not the same. But, again, the mean heights were assumed to be equal in the analysis.

Once the above assumptions were made, both sets of radar data were interpolated to a Cartesian grid. This grid consisted of 81 X 81 X 1 grid points; the location of the SMART radar was the origin of the grid. The grid points were separated every 250 m, making the grid 20 km wide in both horizontal directions. The one vertical level was located at 500 m above ground level. To interpolate the data to a grid, a Cressman scheme was used with a 500 m radius of influence. To synthesize the wind field, a standard iterative dual-Doppler wind-synthesis method was used in Cartesian coordinates. For a more detailed explanation of this method, see Brandes (1977), Ray et al. (1980), or Dowell and Shapiro (2003).

3.2 Dual-Doppler Analysis

The two sets of data were processed by dual-Doppler analysis software. The initial "test" run used data that appeared promising. This test was run to determine initially if the data were viable to use with the analysis software. The time of the chosen scan was 0304 UTC for both the XPOL and SMART radars. This time was chosen because both sets of radar data had clearly defined hook echoes and velocity couplets indicating the strong likelihood that a tornado was on the ground at the time. Figs. 2 and 3 show the results of the initial, preliminary, dual-Doppler analysis.

As was mentioned previously, due to the large number of assumptions and uncertainties associated with both data sets, the analysis is best viewed as a qualitative assessment of the variables plotted. Fig. 2 shows dual-Doppler, horizontal, storm-relative wind vectors plotted along with reflectivity factor. Fig. 3 shows the vertical vorticity that resulted from the analysis in the same location as Fig. 2.

There are a number of readily apparent observations that can be gained from this preliminary analysis. First and foremost is the appendage of reflectivity, usually referred to as the hook echo, that can be seen in Fig. 2. In addition, it is interesting to note the extremely strong wind speeds (relatively speaking) located at the upper right of the figure (near -9.0, 23.0) suggesting strong storm inflow. The quantitative data, which has some degree of error, indicates wind speeds over 50 ms^{-1}. One of the interesting observations noted by many in the vicinity of this storm was the exceptionally strong inflow.

Also of interest is the presence of a strong low-level mesocyclone. The mesocyclone would be expected if, at the time indicated, a tornado was on the ground as is believed for the analysis. This feature is shown in the strong horizontal wind gradient located in the center of Fig. 2 (near -14.0, 18.0), showing the distinct appearance of a strong cyclonic circulation. It is valuable to point out that the largest area of concentrated cyclonic vertical

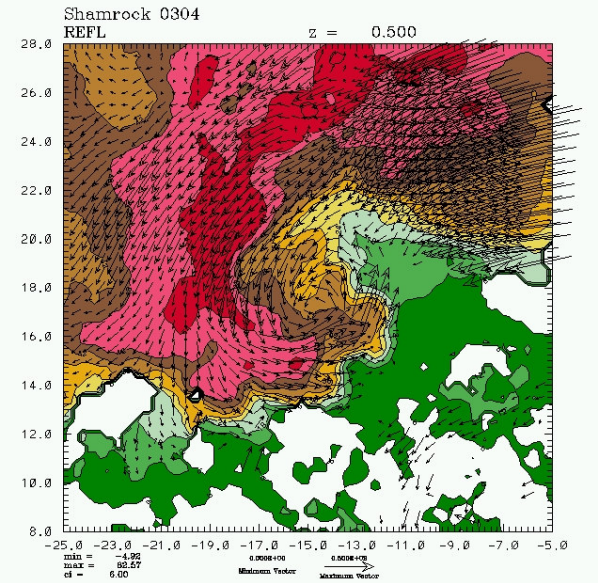

Figure 2. Dual-Doppler analysis showing horizontal, storm-relative wind vectors overlaid on reflectivity factor (dBZ) at 0304 UTC 16 May 2003. Origin indicates location of SMART radar. Reflectivity factor from SMART radar, contoured every 6 dBZ starting with dark green (white is 0 dBZ). Storm motion was estimated as 12 ms^{-1} from 245 degrees.

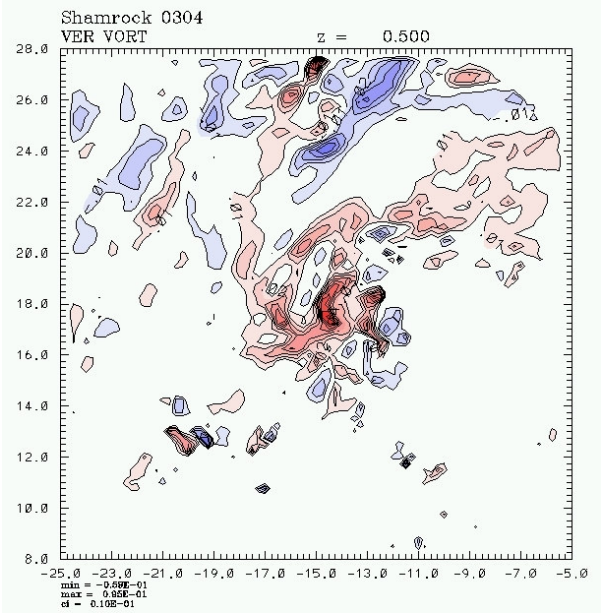

Figure 3. Dual-Doppler analysis showing vertical vorticity contoured every .01 s^{-1} with pink (blue) indicating cyclonic (anti-cyclonic) vertical vorticity at 0304 UTC 16 May 2003. Origin indicates location of SMART radar. Grid used matches that of Fig. 2.

vorticity (Fig. 2) is also centered near the hook (-14.0, 18.0). This observation is somewhat elementary, however, in that there is little disagreement that the stretching of vertical vorticity by the storm updraft provides much of the necessary rotation seen in the low-level mesocyclone, though there is some difference in opinion as to how this vertical vorticity is generated (Rotunno and Klemp 1985; Walko 1993; Wicker 1996). A more detailed look at Fig. 3 shows that the isolines of strong cyclonic vertical vorticity in the location of the low-level mesocyclone are shaped as an annulus. This is consistent with previous observations of an annulus or "horseshoe-shaped" structure to vertical vorticity in the low-level mesocyclone seen in tornadic supercells (Wakimoto and Liu 1998).

In 2003, the UMASS 3-cm radar was fitted with dual-polarization capabilities making it the first mobile, ground-based radar to collect dual-polarization data in supercells and tornadoes. Dual-polarization radars transmit both horizontally and vertically polarized waves and then measure the ratio of the return. It can thus estimate whether the intercepted targets are vertically, horizontally, or spherically oriented through the differential radar reflectivity factor or ZDR. The most practical use of ZDR is to discern between hail and heavy rain when a radar shows high reflectivity factors.

Fig. 4 shows a ZDR image from the UMASS 3-cm radar taken at 0304 UTC on 16 May 2003. This time is the same time as that of the dual-Doppler analysis shown in Figs. 2 and 3. White and yellow colors in the figure indicate high ZDR values which correspond to more oblate or "flat" targets. This would be consistent with large raindrops and, therefore, heavy rain. Lower ZDR values are shown in green and purple and indicate more spherical targets which, in the presence of high reflectivities, are consistent with hail. How these data will aid in helping to understand the structure or formation of tornadoes is still unclear as there is much future work to be done in this area.

At the conference, several additional dual-Doppler analyses will be shown, both prior to and during the development of the tornado, to provide a greater opportunity to analyze not only the parameters shown in the figures, but also how those parameters progress throughout the development of the tornado. Furthermore, any additional pertinent information that can be gained from the ZDR will be discussed.

4. CONCLUSIONS

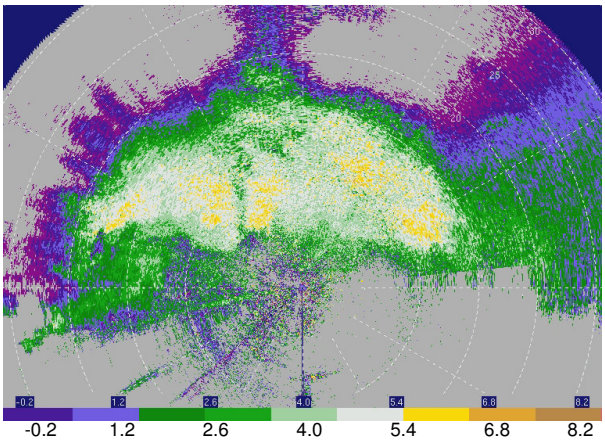

Figure 4. An image of differential radar reflectivity factor (ZDR) from 0304 UTC 16 May 2003 as captured by the UMASS 3-cm radar. Range rings are every 5 km with the location of the XPOL radar at the origin.

The ability to observe tornadogenesis, while rare and difficult to achieve, has been made easier in the last several years with the advancement of ground-based, mobile, Doppler radars. With the increase in the number of such radars, the opportunities for dual-Doppler analyses of tornadogenesis will increase, providing extremely useful observations of the tornadic environment.

In this case, the radars, one a 3-cm Doppler and the other a 5-cm Doppler, were able to capture the life-cycle of an F1 tornado that formed just west of Shamrock, Texas in the evening hours of 15 May 2003. The data from both radars were edited to remove problem areas and, with a variety of underlying assumptions, were analyzed to determine if the results were useful. The analysis software provided storm-relative wind vector data and vertical vorticity that, at least qualitatively, agreed with conventional theory regarding the structures of tornadic supercell thunderstorms.

During the presentation, a more complete dual-Doppler analysis will be given focusing on relevant data taken before and during the formation of the tornado.

5. Acknowledgments

This study was funded by NSF grant ATM - 0241037. Thanks to Curtis Alexander for his damage assessment information regarding this storm and the other relevant data he provided. Thanks also to Dr. Mike Biggerstaff for use of the SMART radar data.

6. References

Biggerstaff, M.I., and J. Guynes, 2000: A new tool for atmospheric research. *Preprints, 20th Conf. Severe Local Storms*. Orlando, FL, Amer. Met. Soc., 277-280.

Bluestein, H. B., S. D. Hrebenach, C. F. Chang, and E. A. Brandes, 1994: Synthetic dual-Doppler analysis of mesoscale convective systems. *Mon. Wea. Rev.,* **122**, 2105-2124.

Bluestein, H. B., A. L. Pazmany, J. C. Galloway, and R. E. McIntosh, 1995: Studies of the substructure of severe convective storms using a mobile 3-mm-wavelength Doppler radar. *Bull. Amer. Meteor. Soc.*, **76**, 2155-2169.

Bluestein, H. B., 1999: A history of severe-storm-intercept field programs. *Wea. and Forecasting*, **14**, 558-577.

Bluestein, H. B., and A. L. Pazmany, 2000: Observations of tornadoes and other convective phenomena with a mobile, 3-mm wavelength, Doppler radar: the spring 1999 field experiment. *Bull. Amer. Meteor. Soc.*, **81**, 2939-2952.

Bluestein, H. B., C. C. Weiss, and A. L. Pazmany, 2003: Mobile Doppler radar observations of a tornado in a supercell near Bassett, Nebraska, on 5 June 1999. Part I: Tornadogenesis. *Mon. Wea. Rev.*, **131**, 2954-2967.

Brandes, E. A., 1978: Mesocyclone evolution and tornadogenesis: Some observations. *Mon. Wea. Rev.*, **106**, 995-1011.

Brandes, E. A., 1977: Flow in severe thunderstorms observed by dual-Doppler radar. *Mon. Wea. Rev.*, **105**, 113-120.

Burgess, D. W., M. A. Magsig, J. Wurman, D. C. Dowell, and Y. Richardson, 2002: Radar observations of the 3 May 1999 Oklahoma City tornado. *Wea. and Forecasting*, **17**, 456-471.

Dowell, D. C., and H. B. Bluestein, 1997: The Arcadia, Oklahoma, storm of 17 May 1981: Analysis of a supercell during tornadogenesis. *Mon. Wea. Rev.*, **125**, 2562-2582.

Dowell, D. C., and H. B. Bluestein, 2002: The 8 June 1995 McLean, Texas, storm. Part I: Observations of cyclic tornadogenesis. *Mon. Wea. Rev.*, **130**, 2626-2648.

Dowell, D. C., and A. Shapiro, 2003: Stability of an iterative dual-Doppler wind synthesis in Cartesian coordinates. *J. Atmos. Oceanic Technol.*, **20**, 1552-1559

Nettleton, L., S. Daud, R. Neitzel, C. Burghart, W. C. Lee, and P. Hildebrand, 1993: SOLO: A program to peruse and edit radar data.

Preprints, *26th Conf. on Radar Meteorology*, Norman, OK, Amer. Meteor. Soc., 338-339.

Oye, R., C. Mueller, and S. Smith, 1995: Software for radar translation, visualization, editing, interpolation. Preprints, *27th Conf. on Radar Meteorology*, Vail, CO, Amer. Meteor. Soc., 359-361.

Pazmany, A. L., F. J. Lopez, H. B. Bluestein, and M. R. Kramar, 2003: Quantitative rain measurements with a mobile, X-band, polarimetric Doppler radar. Preprints, *31st Conf. Radar Meteorology.* Seattle, WA, Amer. Met. Soc., 858-859.

Ray, P. S., C. L. Ziegler, W. Bumgarner, and R. J. Serafin, 1980: Single- and multiple-Doppler radar observations of tornadic storms. *Mon. Wea. Rev.*, **108**, 1607-1625.

Rotunno, R., and J. Klemp, 1985: On the rotation and propagation of simulated supercell thunderstorms. *J. Atmos. Sci.*, **42**, 271-292.

Wakimoto, R. M., and N. T. Atkins, 1996: Observations on the origins of rotation: The Newcastle tornado during VORTEX 94. *Mon. Wea. Rev.*, **124**, 384-407.

Wakimoto, R. M., C. Liu, and H. Cai, 1998: The Garden City, Kansas, storm during VORTEX 95. Part I: Overview of the storm's life cycle and mesocyclogenesis. *Mon. Wea. Rev.*, **126**, 372-392.

Wakimoto, R. M., and C. Liu, 1998: The Garden City, Kansas, storm during VORTEX 95. Part II: The wall cloud and tornado. *Mon. Wea. Rev.*, **126**, 393-408.

Wakimoto, R. M., H. V. Murphy, D. C. Dowell, H. B. Bluestein, 2003: The Kellerville tornado during VORTEX: Damage survey and Doppler radar analyses. *Mon. Wea. Rev.*, **131**, 2197-2221.

Walko, R. L., 1993: Tornado spin-up beneath a convective cell: Required basic structure of the near-field boundary layer winds. *The Tornado: Its Structure, Dynamics, Prediction and Hazards, Geophys. Monogr.*, No. 79, Amer. Geophys. Union, 89-95.

Wicker, L. J., 1996: The role of near surface wind shear on low-level mesocyclone generation and tornadoes. Preprints, *18th Conf. on Severe Local Storms*, San Francisco, CA, Amer. Meteor. Soc., 115-119.

Wurman, J., J. Straka, E. Rasmussen, M. Randall, and A. Zahrai, 1997: Design and deployment of a portable, pencil-beam, pulsed, 3-cm Doppler radar. *J. Atmos. Oceanic Technol.,* **14**, 1502-1512.

Wurman, J., and S. Gill, 2000: Finescale radar observations of the Dimmitt, Texas (2 June 1995), tornado. *Mon. Wea. Rev.,* **128**, 2135-2164.

Wurman, J., 2002: The multiple-vortex structure of a tornado. *Wea. and Forecasting*, **17**, 473-505.

Ziegler, C. L., E. N. Rasmussen, T. R. Shepherd, A. I. Watson, and J. M. Straka, 2001: The evolution of low-level rotation in the 29 May 1994 Newcastle-Graham, Texas, storm complex during VORTEX. *Mon. Wea. Rev.*, **129**, 1339-1368.